Journal of Thermal Biology 62 (2016) 76–83

Contents lists available at ScienceDirect

Journal of Thermal Biology

journal homepage: www.elsevier.com/locate/jtherbio

Self-heating by large insect larvae?

Nikita L. Cooley, Douglas J. Emlen, H. Arthur Woods*

Division of Biological Sciences, 32 Campus Drive HS104, University of Montana, Missoula, MT, 59812, USA

ARTICLE INFO

Keywords:
Heat balance
Body size
Metabolic heat
Critical thermal maxima
Behavioral thermoregulation
Gigantism
Soil

ABSTRACT

Do insect larvae ever self-heat significantly from their own metabolic activity and, if so, under what sets of environmental temperatures and across what ranges of body size? We examine these questions using larvae of the Japanese rhinoceros beetle (*Trypoxylus dichotomus*), chosen for their large size (> 20 g), simple body plan, and underground lifestyle. Using CO_2 respirometry, we measured larval metabolic rates then converted measured rates of gas exchange into rates of heat production and developed a mathematical model to predict how much steady state body temperatures of underground insects would increase above ambient depending on body size. Collectively, our results suggest that large, extant larvae (20–30 g body mass) can self-heat by at most 2 °C, and under many common conditions (shallow depths, moister soils) would self-heat by less than 1 °C. By extending the model to even larger (hypothetical) body sizes, we show that underground insects with masses > 1 kg could heat, in warm, dry soils, by 1.5–6 °C or more. Additional experiments showed that larval critical thermal maxima (CT_{max}) were in excess of 43.5 °C and that larvae could behaviorally thermoregulate on a thermal gradient bar. Together, these results suggest that large larvae living underground likely regulate their temperatures primarily using behavior; self-heating by metabolism likely contributes little to their heat budgets, at least in most common soil conditions.

1. Introduction

Like many ectotherms, insects face the problem of attaining reasonable body temperatures—temperatures that permit adequate performance, including feeding, growth, and reproduction—in environmental conditions that vary in space and time. In cool environments, insects may live far down on the left sides of their thermal performance curves (Deutsch et al., 2008). For insects in such a situation, there are exponential increases in performance to be gained by finding ways to achieve higher body temperatures. Insects often do so using behavioral thermoregulation (May, 1979; Heinrich, 1993), which involves moving through locally available mosaics of microsites and choosing sets of conditions that give higher body temperatures (Bakken, 1992). For individual insects, this is equivalent to choosing sites that increase inputs, and decrease outputs, to its heat budget—for example, by choosing microsites with relatively high air temperatures, high levels of incoming visible and infrared radiation, and relatively warm nearby objects (Woods et al., 2015) or that give low rates of heat loss by evaporation and convection (Gates, 1980). In hot environments, by contrast, the problem is to avoid body temperatures so high that the insect's performance is declining. In such environments, the insect needs to decrease inputs of heat and, if possible, increase outputs. In general, actively seeking out cooler conditions also involves behavioral thermoregulation.

Insects may also warm themselves up significantly using heat produced by their own metabolism. Whether they do so depends primarily on mass-specific intensity of metabolism, body size, and rates of heat loss, which are lower across well-insulated surfaces. Birds and mammals, most of which have high mass-specific metabolic rates and large body sizes (compared to insects), are the consummate endothermic homeotherms. Most produce enough heat to sustain constant body temperatures in the range of 35–40 °C. Insects of course are smaller and, with some significant exceptions (see below), have mass-specific metabolic rates that are an order of magnitude or more lower per unit body mass than those of birds and mammals (Robinson et al., 1983); in general, their body temperatures are much more closely coupled to ambient environmental conditions. Much of the time, they are ectothermic poikilotherms. Even so, it may be possible for insects to produce significant metabolic heat. The best examples are large flying adults, which can have extraordinarily high mass-specific metabolic rates (Bartholomew and Casey, 1978). Adults of several species of moths maintain thoracic temperatures above 38 °C when flying, which is possible because their thoracic muscles produce heat at such high rates (Heinrich, 1970; Casey, 1981). Indeed, some flying insects produce so much metabolic heat that they risk overheating (Heinrich, 1980, 1993); the difficulty then is to shed heat rapidly enough. This

* Corresponding author.
E-mail address: art.woods@mso.umt.edu (H.A. Woods).

http://dx.doi.org/10.1016/j.jtherbio.2016.10.002
Received 26 April 2016; Received in revised form 8 October 2016; Accepted 16 October 2016
Available online 17 October 2016

may explain why some large beetles and moths fly only at night.

Because holometabolous insect larvae do not power locomotion nearly as intensely as adults, their mass-specific metabolic rates while active generally are much lower. For example, a fifth-instar caterpillar of *Manduca sexta* consumes 30–50 μmol O_2 g^{-1} h^{-1} (Greenlee and Harrison, 2005) whereas an adult *M. sexta* in free flight consumes about 2 mmol g^{-1} h^{-1} (Heinrich, 1971a), which is 40 – 65× greater on a mass-specific basis. Nevertheless, several factors may allow larvae to self-heat. First, larvae generally have simple sac-like bodies, with relatively small ratios of surface area to volume and therefore relatively small surfaces across which to lose heat. Second, not all larvae have low mass-specific metabolic rates; for example, some herbivorous caterpillars feed and digest at very high rates, with that activity supported by high mass-specific rates of metabolism (Kingsolver and Woods, 1997). Third, larvae of some species can grow to very large absolute body sizes (always larger than the adults into which they metamorphose). Large insects generally have higher absolute metabolic rates (Chown et al., 2007) and thus produce more metabolic heat, possibly causing them to self-heat to greater extents. Fourth, larvae of many species live in confined spaces—underground, in rotting vegetation or wood, in constructed shelters—where there is little potential for evaporative or convective cooling (for example of bird eggs in such an environment, see Seymour and Bradford, 1992). In effect, those confined spaces can act as insulation.

We examine the potential for larval self-heating using the Japanese rhinoceros beetle (*Trypoxylus dichotomus*), which occurs in Japan, Taiwan, Korea and eastern China. On Honshu island, Japan, where these animals have been best studied, adult males defend wounds on the sides of *Fraxinus* sp. and other trees, which serve as feeding sites (Hongo, 2007a, 2007b; McCullough, 2012). Females visit these territories to feed and mate with males, leaving later to lay eggs in the soil near decaying humus (Karino et al., 2004). Eggs are laid between July and September, and larvae feed below ground until June – July of the following year (Plaistow et al., 2005). As they feed, larvae orient towards high concentrations of CO_2 (Kojima, 2015), which appears to lead them towards high quality, or especially fermented, humus. This also can lead to large aggregations of larvae (Kojima et al., 2012, 2014; Kojima, 2015), at depths down to 25 cm in the soil. At the end of their final (3rd) larval instar, animals construct brittle pupal cells, which are vulnerable to damage by other burrowing larvae.

Because of their extreme size, and the fact that they develop underground in decomposing—hot—organic matter, *Trypoxylus* larvae may be prone to overheating. First, larvae can reach over 30 g (D. Emlen, personal observation). If any larvae self-heat as a result of high metabolic rates and large body size, these are likely candidates. Second, their soil microhabitats provide little potential for evaporative or convective cooling and may insulate larvae from rapid heat loss by conduction. Using flow-through and thermolimit respirometry (Lighton and Turner, 2004), we measured larval metabolic rates and values of CT_{max}. In addition, we examined the ability of larvae to behaviorally thermoregulate on a thermal gradient bar. Lastly, we developed and analyzed a mathematical model of larval heat balance that predicts increases in body temperature from self-heating. We used the model to evaluate self-heating in soils of different temperatures and across a set of realistic body sizes. Finally, we extended the model to ask how much very large insect larvae (larger than extant) would self-heat.

2. Materials and methods

2.1. Animals

Larvae of the Japanese rhinoceros beetle were purchased from a commercial insect distributor (Yasaka Kabuto Kuwagata World, Hamada City, Japan) and reared to adulthood in the laboratory. Individuals were placed in plastic jars (1 L) containing substrate made from a 1:1 mixture of organic hardwood compost (Hiroki Gotoh, personal communication) and quick-fermented hardwood sawdust (Emlen et al., 2012). Additionally, eggs were collected from a local laboratory colony and allowed to grow to the third instar. 110 larvae were collected and placed in plastic jars (1 L) containing the previously described substrate mixture. We kept approximately 50 larvae at room temperature (22 °C) and another 60 in a temperature-controlled growth chamber at 10 °C to postpone pupation. Larvae were pulled from the growth chamber as needed and held at room temperature for 24 h before being used in experiments.

2.2. Larval metabolic rates

We estimated larval metabolic rates from rates of carbon dioxide emission, using flow-through respirometry. CO_2 levels were measured by an infrared gas analyzer (LI-7000, LI-COR, Lincoln, Nebraska) set up in differential mode. In this mode, dry, CO_2-free air from a cylinder of compressed breathing air (Norco, Boise, ID, USA) was first passed through the instrument's reference side, then past the larva and returned to the instrument's measurement side. The gas analyzer was calibrated using pure N_2 and 2000 parts per million (p.p.m.) CO_2 in N_2 (NorLab, Boise, ID, USA). Flow rates of gas were 200 mL min^{-1} (STP) and were regulated by a mass flow controller (Unit UFC-1100, 500 mL min^{-1} maximum flow rate, Yorba Linda, CA), which was controlled by a separate set of electronics (MFC-4, Sable Systems). The flow controller was recently calibrated at the factory, and we checked its flow at 200 mL min^{-1} against a bubble flow meter. Analog signals from the LI-7000 were sent to an A/D converter (UI2, Sable Systems) and then recorded using the ExpeData software (Sable Systems). Rates of CO_2 emission were converted to L min^{-1} O_2 consumption assuming a respiratory exchange ratio of 0.70 (Chown et al., 2007) and then transforming to μW of heat output using the conversion of 19.7 kJ L^{-1} of O_2 consumed (Schmidt-Nielsen, 1997) ×60 s min^{-1}×10^9 μJ kJ^{-1}. Errors in estimates of the heat output per unit O_2 consumed will lead to an error of at most 7% in rate of heat production.

Carbon dioxide emission was measured for ten rhinoceros beetle larvae at room temperature (22 °C). Each larva was taken from its rearing jar (no prior period of food deprivation) and placed into a horizontal 110-mL cylindrical glass chamber (length 160 cm, diameter 3 cm) sealed by a Teflon end cap with two built-in O–rings. Air entered through a hole in the end cap and exited at the other end through a drawn out taper in the glass that was connected to Bev-a-line tubing, so that the chamber was flushed approximately twice per minute. Larvae were weighed and placed in the chamber 5–10 min prior to measurement to allow them to settle down. Sexes were unknown. Each larva's CO_2 output was measured for 15 min, during which time it was free to move. Movement had only slight effects on CO_2 emission, probably because movements themselves are very slow. CO_2 measurements were reported as the average p.p.m. for the last 7 min of each experiment. Because the larvae were not post-absorptive and we included periods during which they were moving, the metabolic rates derived from these measurements are neither resting nor standard; rather, they reflect digestion, absorption, and moderate activity. These conditions are the most appropriate for estimating rates of heat output during normal activity in the field.

2.3. Critical thermal maxima

The CT_{max} was determined for six larvae using thermal ramping. Because these beetle larvae are some of the largest insects ever measured, some in excess of 25 g, we developed a protocol based on work by Terblanche et al. (2007) and using the thermolimit analysis proposed by Lighton and Turner (2004) (see below). The primary considerations were to ramp slowly enough that larval body temperatures were in thermal steady-state with the temperature of the air in the

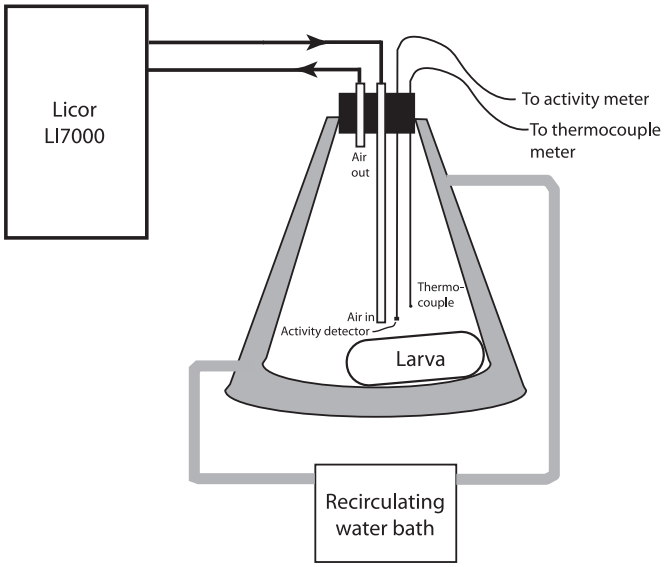

Fig. 1. Schematic of apparatus for larval ramping experiments. Larvae were ramped in a water-jacketed flask whose temperature was set by a programmable temperature-controlled recirculating water bath. Carbon dioxide emission was measured using a flow-through system, temperature was measured by a type-T thermocouple, and activity was monitored by an infrared motion detector.

flask, but quickly enough to reduce the effects of accumulated exposure to high but sublethal temperatures and to the experimental apparatus (Rezende et al., 2011). To determine a good ramp rate, test ramps were performed in which a larva was placed in the chamber with one thermocouple taped to the cuticle and another measuring the surrounding air temperature in the chamber. We decided to use a ramp rate of 0.08 °C min^{-1}, which was fast enough that individual ramps could be done in approximately 6 h but slow enough that larvae were largely in thermal steady-state with the flask air. However, even at this slow ramping rate, body temperatures of the larvae lagged 1–1.5 °C behind air temperature. It is unclear whether the temperature lag reflected larval thermal inertia or evaporative cooling from the cuticle. In general, rates of transcuticular evapotranspiration in insects are small, although they could be higher in soil-dwelling stages, like larval *Trypoxylus*, that are normally exposed to high ambient relative humidities. The temperature ramp began at 20 °C and ended at 50 °C, giving a total ramp time of 6 h and 25 min

Larvae were ramped individually in a 250-mL, water-jacketed, glass Erlenmeyer chamber (see Fig. 1). The chamber was attached to a programmable Polystat® temperature-controlled recirculating water bath (Cole-Parmer). During each ramp, we measured rates of CO_2 emission (using the system described above), actual air temperature, and levels of activity by the larva. Flow rates of dry air were 350 mL min^{-1}, with air directed in through a metal cannula in the rubber stopper and then through a plastic tube to the bottom of the flask; outgoing air went out through another metal cannula that just pierced the stopper. Temperature was measured by a type T thermocouple inserted into the flask's stopper through a small hole and attached to a thermocouple meter (TC-1000, Sable Systems). Levels of activity were monitored using an infrared activity detector (AD-2, Sable Systems) modified so that the emitter and detector both were mounted on long wires. The wires were glued into the flask stopper so that the emitter and detector both were positioned about 1 cm above the larva. Activity was monitored in 4 of the 6 individual ramps. To identify CT_{max}, we used Lighton and Turner's (2004) approach. As an insect's temperature rises, it eventually undergoes rapid physiological change (identified as CT_{max}) during which (simultaneously) rates of CO_2 emission fall sharply, gross motor movements cease, and control over the spiracles is lost (CO_2 trace suddenly stops showing high-frequency fluctuations). To aid in identifying these breakpoints, we also calculated the absolute difference sums (ADS) of both the CO_2 emission and activity data for each larva (Lighton and Turner, 2004).

2.4. Behavioral thermoregulation experiment

In order to test whether larvae adjusted their body temperature by moving to warmer or cooler locations, we exposed them to composted substrate distributed on a custom-built thermal gradient bar. The bar was constructed from a 20-kg block of aluminum of dimensions 0.914 m (length)×0.305 m (width)×0.0254 m (thickness). Temperatures at the two ends of the bar were fixed by circulating temperature-controlled water through 13 mm diameter threaded holes drilled completely through each end across the width. Water temperature was regulated using a programmable Polystat® temperature controlled recirculating bath (Cole-Parmer) and a digital refrigerated recirculating chiller (VWR Scientific). The temperature on one end was set to 5 or 10 °C, while the other end was set to 50 °C. The aluminum block was insulated on the bottom and sides by pieces of Styrofoam. The surface was divided into four lanes using 2.54 cm tall Plexiglas dividers to restrict each larva to lengthwise movement and keep the larvae from interacting. Lanes were filled with 2–3 cm depth of a dry 1:1 mixture of organic hardwood compost and quick-fermented hardwood sawdust substrate that was allowed to equilibrate to the linear gradient temperature. While they were moving in the substrate, larvae were in direct contact with the aluminum.

To ensure that we had created a linear thermal gradient in only the lengthwise direction, 16 type T thermocouples were inserted into 3 mm diameter holes drilled into the underside of the aluminum block. The thermocouple holes were distributed along the middle of the aluminum block every 11.43 cm, as well as across the block (in two places) every 6.1 cm. To ensure good thermal contact, holes were first filled with thermal paste. The steepness of the gradient was 0.4 °C (range 0.39–0.44) per cm. A total of 35 larvae was used to determine temperature preference along this thermal gradient, while 28 larvae were used in control runs (constant temperature of 22–22.5 °C everywhere in the arena).

Individual larvae were introduced into the gradient bar facing a random direction. Runs were video-recorded from above using a webcam. The larvae displaced substrate as they traveled along their lane, which allowed us to observe their movements from the camera. Recordings lasted either 1 or 2 h, and still images were recorded every 10 s. These images were analyzed in ImageJ using a manual tracking plugin, allowing us to track the paths of each individual larva. We then converted each position to an environmental temperature.

2.5. Analytical model of larval heat balance

A key aspect of our study is to ask about the thermal biology of larvae in the size range we studied (up to approximately 30 g) and of larvae larger than those that we measured directly. We approached this problem by extrapolating from our measured values—by scaling them up to hypothetical large larvae. The two specific questions were: (1) Do larvae of *T. dichotomus* produce enough metabolic heat to warm themselves significantly underground? (2) More generally, how big must underground insects evolve to be before heat from their own metabolism raises their temperatures significantly?

To analyze these questions, we developed a model of larval heat balance. Larvae are modeled as metabolizing cylinders of length L and diameter D buried at depth z in the soil (Fig. 2). For an animal in soil, the heat generated is equal to the heat lost by conduction to the soil and the heat stored in its tissues:

$$Q_{gen}=Q_{cond}+Q_{st}. \quad (1)$$

The core-skin temperature gradient for a cylindrical object with distributed heat generation (Bird et al., 2002) is

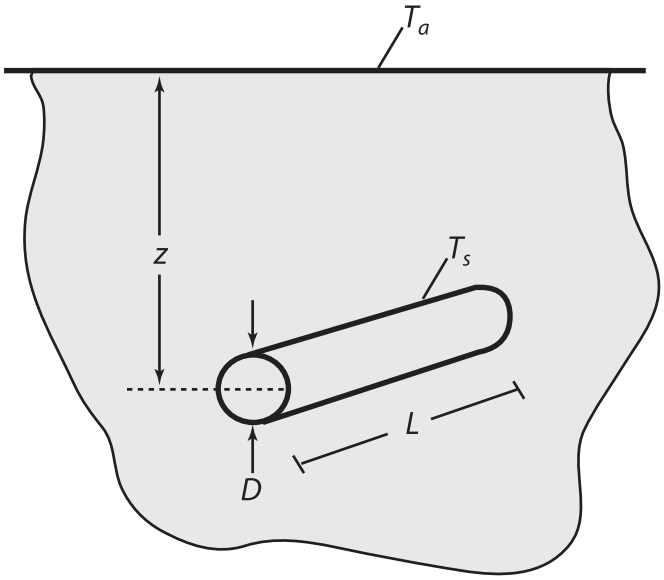

Fig. 2. Schematic of a larva in soil. The larva is idealized as a cylinder of length L and diameter D positioned at depth z below the surface of the soil. The larva has surface temperature T_s and the soil surface has temperature T_a.

$$T_c - T_s = \frac{qR^2}{4k_L} \tag{2}$$

where q is the heat generated per unit volume, $q = Q_{gen}/V$ and k_L is the conductivity of larval flesh. Multiplying both sides by V and rearranging gives

$$Q_{gen} = \frac{4k_L V (T_c - T_s)}{R^2}. \tag{3}$$

Conduction from the cylinder is described by

$$Q_{cond} = S_F k_S (T_s - T_a) \tag{4}$$

where S_F is a shape factor, $S_F = \frac{2\pi L}{\ln(4z/D)}$, with the constraints that $L \gg D$ and $z > 3D/2$.

The heat stored is given by

$$Q_{st} = mc_p \frac{dT_c}{dt} \tag{5}$$

where m is mass, c_p is the heat capacity of the larva, and dT_c/dt is the rate of change in body temperature.

Substituting the definition of each term into Eq. (1) gives

$$\frac{4k_L V (T_c - T_s)}{R^2} = S_F k_S (T_s - T_a) + mc_p \frac{dT_c}{dt}. \tag{6}$$

Solving for dT_c/dt and substituting $T_s = T_c - \frac{qR^2}{4k_L}$ leads to

$$\frac{dT_c}{dt} = \frac{1}{mc_p}\left[S_F k_S \left(\frac{qR^2}{4k_L} + T_a - T_c\right) + \frac{V 4k_L}{R^2}\left(T_c - \left[T_c - \frac{qR^2}{4k_L}\right]\right)\right] \tag{7}$$

which simplifies to

$$\frac{dT_c}{dt} = \frac{1}{mc_p}\left[S_F k_S \left(\frac{qR^2}{4k_L} + T_a - T_c\right) + Q_{gen}\right]. \tag{8}$$

Finally, because metabolic generation of heat itself depends on body temperature, we make q and Q_{gen} functions of T_c:

$$\frac{dT_c}{dt} = \frac{1}{mc_p}\left[S_F k_S \left(\frac{q(T_c)R^2}{4k_L} + T_a - T_c\right) + Q_{gen}(T_c)\right]. \tag{9}$$

2.5.1. Solving Eq. (9)

Eq. (9) is a differential equation, which approaches a steady-state body temperature $dT_c/dt = 0$ over time if the external conditions are stable and metabolic heat generation is constant. We found this steady-state body temperature using the *ode* function from the *deSolve* package (Soetaert et al., 2010) in R. The temperature-dependence of Q_{gen} was modeled by introducing a temperature factor describing the factorial increase in metabolic rate as body temperature rises above 20 °C (see Supplemental Fig. 1). The relationship between metabolic rate and body temperature was a fitted sigmoid derived from the mean values of metabolic rate calculated from the ramping experiments used to establish CT_{max}.

2.5.2. Assumptions

The model above makes seven key assumptions. (1) The beetle larva is cylindrical and is in direct contact with the soil surrounding it. In fact, beetles often curl into more compact masses. Larvae do not excavate large air-filled chambers; usually a significant proportion of the larval cuticle is in contact with the surrounding soil. (2) Beetle larvae stay in the same location in the soil until they reach steady-state body temperatures, and the soil temperature profile itself is unchanging. Because Eq. (9) describes transient changes in body temperature, these assumptions could be relaxed in a more elaborate analysis. (3) Levels of O_2 and CO_2 in the soil do not alter or limit rates of metabolism by larvae. For most larvae most of the time, this will be true. Gas levels in soils generally match the composition of local air aboveground, as long as the soil is relatively dry. In wet soil, high rates of soil respiration together with low rates of gas transport can give low levels of O_2 and high levels of CO_2 (Campbell and Phene, 1977; Greenway et al., 2006). In large piles of rapidly fermenting soils (compost), levels of CO_2 can reach 2 – 4% and O_2 levels are drawn down by the same amount (Macgregor et al., 1981). For resting insects, the critical partial pressure of O_2 (below which metabolism is depressed) is usually quite low—on the order of 3–5 kPa O_2 (Harrison et al., 2014)—suggesting that low O_2 generally will not be a problem. High levels of CO_2 may cause greater physiological disturbance, by anaesthetizing larvae and leading to long-term metabolic changes (Colinet and Renault, 2012). (4) All heat transfer in the soil is by conduction, not by the evaporation, transport, and condensation of water vapor, which has been shown (Westcot and Wierenga, 1974) to account for a significant fraction of heat flux in soil. The errors introduced by this assumption likely are small, because the methods used to determine soil conductivity (see Seymour and Bradford, 1992; Ahn et al., 2009) include the effects of water vapor fluxes; in other words, the effects of water vapor transport, while not explicitly included in our model, are captured in the range of values of k_S we used. (5) Heat transport inside larvae is by conduction, not circulation of the hemolymph. Clearly some heat will be moved by hemolymph, and this could be modeled using higher effective k_L (> 0.5 W C^{-1} m^{-1}). (6) Larval metabolic rate depends on T_c, not on the temperature gradient between T_c and T_s. (7) Larval density and aspect ratio are invariant across body sizes.

2.5.3. Parameter values

All parameters are defined in Table 1. Larval volume was calculated as $V = m/\rho = \pi R^2 L$. In addition, we assumed a constant larval aspect ratio $A = \frac{L}{D} = \frac{L}{2R}$ of 5, which was estimated from a photograph of larval *T. dichotomus* in Fig. 1b of Kojima et al. (2014). Thus, $L = 2RA$ and $R = \sqrt{V/2\pi A}$.

We measured metabolic rates at room temperature (25 °C) for larvae of a range of body masses. Measured metabolic rates fell neatly onto the metabolic scaling lines fitted by Chown et al. (2007) to 391 insect species. Those fitted lines (ordinary least-squares and phylogenetically-corrected) had means values of 0.82 and 0.75, respectively, and their joint confidence interval was 0.70 – 0.85. We therefore used 0.75 as the core scaling value. The effects of temperature on metabolic rate were incorporated by fitting a sigmoid to the mean temperature-response curve (between 20 and 45 °C) measured in our tempera-

Table 1
Definitions, values, and units of parameters used in the model[a].

Parameter	Definition	Value (range)	Units
b	Scaling exponent of metabolism	0.75	dimensionless
m	Mass	20 – 2000	g
M	Metabolic rate	variable	W
A	Aspect ratio of larva (L/D)	5	dimensionless
R	Radius of larva	0.00876 – 0.0406	m
D	Diameter of larva	$2R$	m
L	Length of larva	0.0876 – 0.406	m
V	Volume of larva	$2.1 \times 10^{-5} - 2.1 \times 10^{-3}$	m^3
z	Depth of larva in soil	0.05 – 0.25	m
ρ	Density	950	$kg \cdot m^{-3}$
k_S	Thermal conductivity of larva	0.5	$W \cdot °C^{-1} \cdot m^{-1}$
k_L	Thermal conductivity of soil	0.06 – 0.6	$W \cdot °C^{-1} \cdot m^{-1}$
c_p	Heat capacity of larva	3421	$J \cdot °C^{-1} \cdot kg^{-1}$
T_a	Temperature of the surface of the soil	15 – 30	°C
T_s	Temperature surface of the larva	variable	°C
T_c	Temperature core of the larva	variable	°C

[a] For 'compost soil blend' described in Ahn et al. (2009). Low values are for compost with very low water content, and high values for high water content.

ture-ramping experiments. Values for the thermal conductivity of soil (k_S) were based on empirically measured values for composted soil (Ahn et al., 2009). These values differ depending on the water content of the compost. For the core calculations, we used values from the middle of the range.

3. Results

3.1. Larval metabolic rates

The 10 larvae used in this experiment had average masses of 21.1 ± 3.5 g (mean ± S.E.M., range 15.2–26.3 g; Fig. 3). The linear regression slope of metabolic rate on body mass was not significantly different from zero or from one, using a linear model (confidence interval =−0.127–1.507) and ANOVA test (P=0.087), and so it is not included.

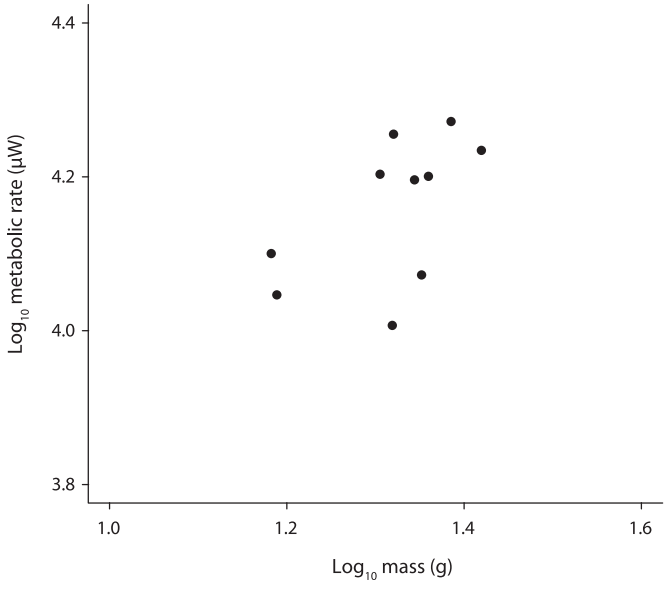

Fig. 3. Metabolic rates of larval *Trypoxylus dichotomus*, estimated from rates of CO_2 emission. Larval masses ranged from 15.4 to 26.3 g. In this small dataset, there was no significant relationship between mass and metabolic rate.

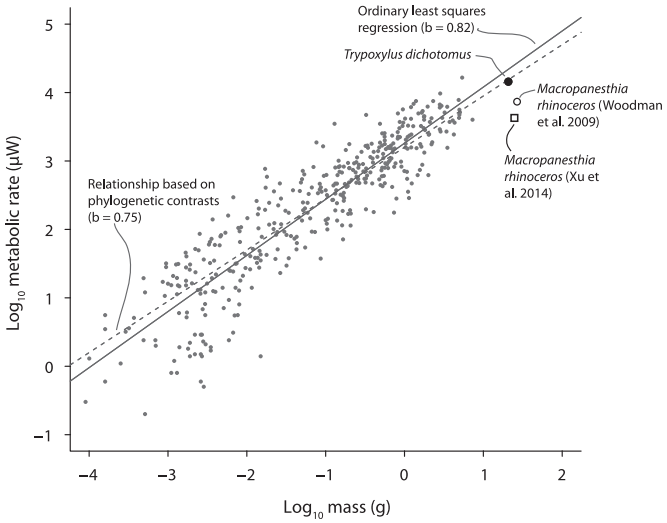

Fig. 4. Mean mass and metabolic rate of *T. dichotomus* (black dot) plotted together with a sample of insect metabolic rates (primarily standard metabolic rates) from 391 species compiled and analyzed by Chown et al. (2007) and data on resting metabolic rates of the giant burrowing cockroach *Macropanesthia rhinoceros* (Woodman et al., 2007; Xu et al., 2014). Fitted lines are from Chown et al. (2007). Solid line: $\log_{10}$ metabolic rate =3.26+0.82× $\log_{10}$ body mass; dotted line: $\log_{10}$ metabolic rate =3.20+0.75× $\log_{10}$ body mass. Metabolic rates of *M. rhinoceros* are lower than for *T. dichotomus* in part because the cockroaches were post-absorptive. In addition, the measurements by Xu et al. (2014) carefully excluded periods of movement.

This is most likely because of the variation and small sample size.

The average mass and metabolic rate were used to compare our data to previous insect data on standard metabolic rates compiled by Chown et al. (2007) and for another giant insect, the Australian burrowing cockroach *Macropanesthia rhinoceros*, measured by Woodman et al. (2007) and Xu et al. (2014). While Chown et al. (2007) scaled all the metabolic rates to 25 °C, our data was taken at 22 °C and was not significantly altered by scaling to 25 °C, so we left the data uncorrected. Woodman et al.'s data on *M. rhinoceros* were interpolated to 25 °C using measured values at 20 and 30 °C; Xu et al.'s data are for resting metabolic rates taken at 25 °C. It is clear (Fig. 4) both that, along with adults of *M. rhinoceros*, larvae of *T. dichotomus* are the largest insects measured to date and that their metabolic rates fell close to the expected values from extrapolating standard metabolic rates from other insects (recall that metabolic rates of *T. dichotomus* include digestion, absorption, and movement). This suggests that it is reasonable to project out metabolic rates of insects larger than actually observed in nature for our mathematical model.

3.2. Critical thermal maxima

Six larvae were exposed to thermal ramping to determine critical thermal maxima. A representative recording is shown in Fig. 5. During the temperature ramps, patterns of CO_2 emission by larvae showed several typical characteristics: a gradual increase in CO_2 output followed by one or two peaks and valleys, then followed by a final peak, after which CO_2 emissions declined rapidly and smoothly, indicating complete loss of muscular control and death.

In most recordings, CO_2 emission declined during the first 15–20 min after the larva was introduced into the chamber, likely reflecting that larvae were initially stressed by handling but then became accustomed to their surroundings. After this, metabolic rate gradually increased between 25 and 35 °C. The first peak occurred between 35–40 °C. In some cases, a second, smaller peak appeared before the final peak. The final peak occurred between 45 and 48 °C (the six larvae had CT_{max} of 45, 45.5, 46, 47, 48, 48 °C), after which there was a steady decline. Because larval temperature was consistently 1–1.5 °C below air temperature, larva CT_{max} occurred between 44–

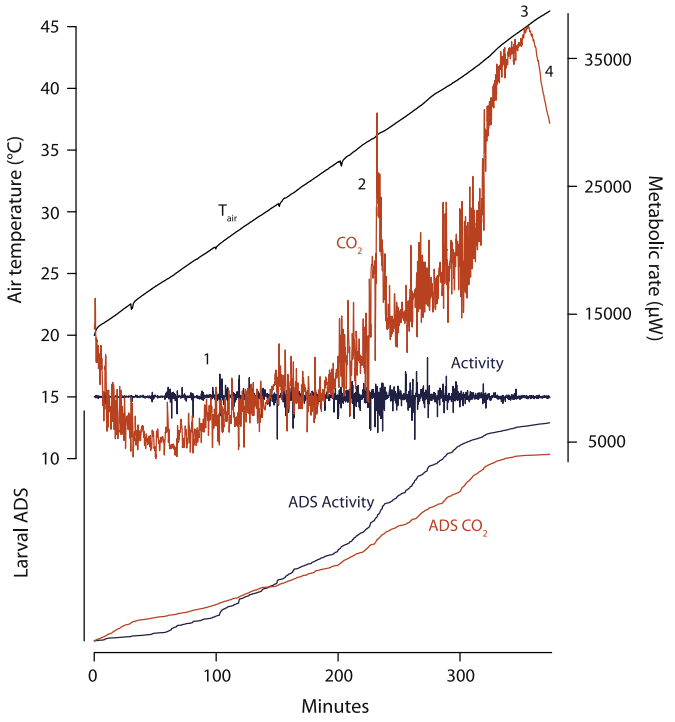

Fig. 5. Typical traces showing larval activity (blue line) and CO_2 emission (orange line) during a temperature ramp, along with (lower panel) cumulative absolute difference sums (ADS). Activity was recorded using an infrared sensor, which outputted voltage spikes when the larva moved; because there is an arbitrary relationship between magnitude of movement and magnitude of the spikes, the activity trace is plotted without units. In addition, ADS curves are plotted without units because what matters is the shape of the cumulative curve, not their actual magnitudes. Together, this information can be used to estimate CT_{max}. In particular, the plot shows (1; 20–35 °C) a gradual increase in metabolic rate with temperature followed by a peak and a valley (2; 35–40 °C). Subsequently, there is (3; 45–48 °C) a final peak ending with a (4; > 45–48 °C) steep decline. For this larva, CT_{max} is estimated to be 45 °C, reflecting that CO_2 emission reaches a maximum at this temperature while activity levels fall sharply. In addition, the emission trace becomes smooth at high temperatures, indicating that the larva has lost control of its spiracles.

47 °C.

3.3. Behavioral thermoregulation experiment

Preliminary experiments revealed that larvae may have been attracted to light coming from a window in the lab. To control for these effects, we performed experiments with the thermal gradient oriented in both directions (hot end both toward and away from ambient light).

Larval position on the bar depended strongly on whether or not they were exposed to a thermal gradient. In the absence of a gradient, larvae spent time at a relatively wide range of positions on the bar, but clearly preferred the side toward ambient light (Fig. 6). When the light came from the left (Fig. 6A), larvae strongly preferred the left side, as judged by sampling 358 times (~1 h) from the mean density distribution (*t*-test, t=−5.29, df =357, P < 0.0001). When the light came from the right (Fig. 6B), larvae preferred the right side (t.test, t=32.8, df =357, P < 0.0001). By contrast, larvae exposed to the thermal gradient strongly preferred temperatures of 28 – 30 °C (grey dotted lines in Fig. 6A, B). In both cases, the mean spatial distributions of these larvae differed from those of the control larvae (two-sample Kolmogorov-Smirnov test using 358 data points resampled from the mean density distributions; for light from the left D =0.444, P < 0.0001; for light from the right D =0.408, P < 0.0001). In the two experiments, the maximum density (temperature at which the larvae spent the most time) was 28.6 °C ± 1.87 (SEM, N =15) and 29.0 °C ± 1.27 (SEM, N =20). Thus, larvae preferred temperatures near 29 °C.

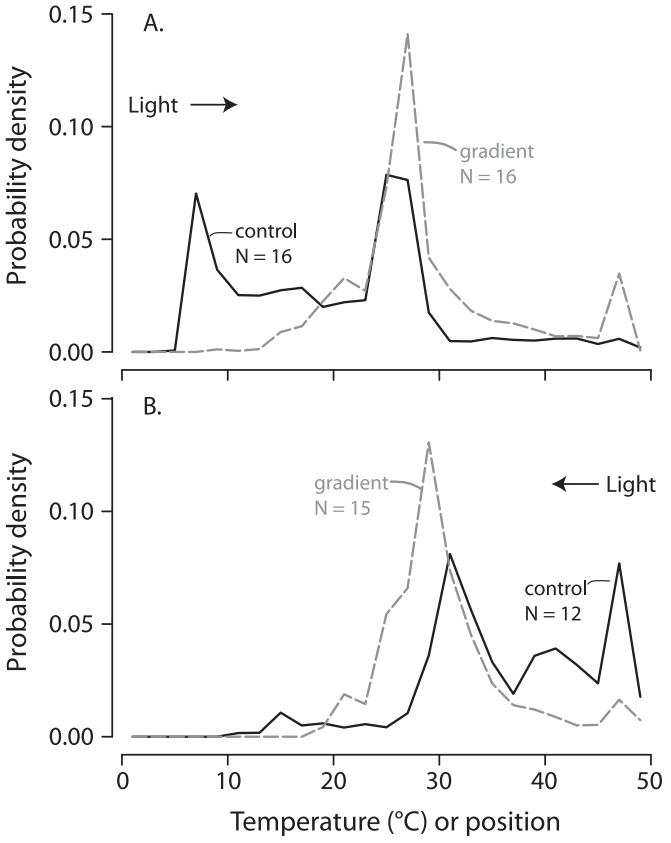

Fig. 6. Histograms of larval positions on the thermal gradient bar when (A) the ambient window light was coming from the left and (B) from the right. Histograms were calculated as the mean densities of each individual larva's histogram (position sampled every 10 s for 1 or 2 h). In each panel, the grey dashed line indicates larval distributions when there was a thermal gradient; the black line indicates when there was no thermal gradient. Thus the x-axis indicates either temperature or position, depending on treatment.

3.4. Analytical model of larval heat balance

Our model shows that, for larvae within the size range of extant insects (< 100 g), temperature increases due to metabolic rate are not expected to increase larval temperature more than about 2 °C above soil temperature (Fig. 7A, B). The main factors affecting the temperature excess above soil temperature are depth in the soil and the thermal conductivity of the soil—greater depths and lower thermal conductivities gave higher steady-state body temperatures, all else being equal. Low thermal conductivities are possible in dry soils (Ahn et al., 2009), which contain a lot of insulating air spaces. Even a modest increase in moisture, however, can raise soil thermal conductivity (k_S) to 0.2 $W{\cdot}°C^{-1}{\cdot}m^{-1}$ or greater. In such soils, heat is conducted more rapidly away from its source (the larva), giving a lower steady-state body temperature. As body size increases up to 2000 g (2 kg), larvae begin to self-heat more significantly, again depending on a number of factors. The highest level of self-heating (> 6 °C) was for the largest larvae in warm (30 °C), dry soil (low k_S). Higher soil temperatures shift the entire larval metabolic curve up, so that relatively more self-heating occurs in hotter soils.

4. Discussion

We used the large larvae of the Japanese rhinoceros beetle (*Trypoxylus dichotomus*) to examine the relative roles of behavioral thermoregulation (May, 1979; Heinrich, 1993) and metabolic self-heating in setting body temperatures. We estimated heat production from measurements of CO_2 emission and assessed the ability of larvae

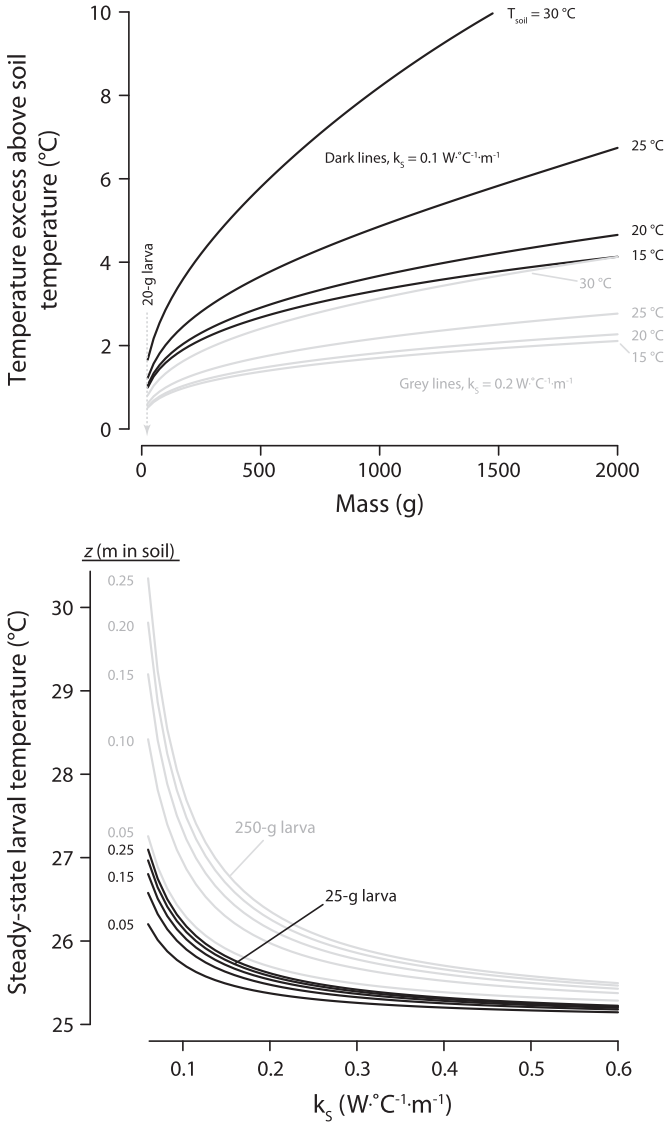

Fig. 7. Main result of the model of larval heat balance. (A) Steady-state temperature excess of larvae above the temperature of the soil for combinations of four soil temperatures and two soil thermal conductivities (dark versus grey lines). Higher soil temperatures give greater excesses because warmer larvae produce more metabolic heat. (B) Joint effects of depth in the soil and soil thermal conductivity on the steady-state body temperatures of a 25 g and a 250 g larva.

to choose positions on a thermal gradient bar, and we generalized our findings using a mathematical model. Collectively, our results suggest that large, extant larvae (20 – 30 g body mass) can self-heat by at most 2 °C, and under many common conditions (shallow depths, moister soils) would self-heat by less than 1 °C. Larvae appear capable of modifying their body temperatures much more significantly by behavioral thermoregulation. These results are robust because, in essence, we stacked the deck in favor of finding an effect—by using one of the largest larvae commercially available, which has a particularly low surface-area-to-volume ratio for its size and which lives in decaying soil without access to modes of heat loss that many other terrestrial insects can use, such as convection and evaporation (Church, 1960; Prange, 1996). Moreover, active metabolic rates of larval *T. dichotomus* are not particularly low for their size; they fall close to the scaling line established from meta-analyses of mostly standard metabolic rates of other, smaller insects (Chown et al., 2007). Thus, if any 30-g larva was going to self-heat, *T. dichotomus* is a good candidate; they self-heat modestly at best, and the model suggests this is so for larvae even substantially larger than the ones we used.

There are few data in the literature available for comparison to our results. The most relevant are several studies of brush turkey (*Alectura lathami*) and mallee fowl (*Leipoa ocellata*) eggs (Vleck et al., 1984; Seymour et al., 1987; Seymour and Bradford, 1992), which are incubated in large mounds of soil and leaf litter whose decomposition provides heat to the eggs. In a lab experiment on one brush turkey egg and several mallee fowl eggs, Seymour et al. (1987) showed that late-stage eggs had shell temperatures of 2.8 (brush turkey) or 1.9 °C (mallee fowl) higher than surrounding soil. Compared to values predicted by our model, these temperature increments are quite low—especially given that the eggs are about 175 g and have metabolic rates (at 34 – 36 °C) that are about 335 mW (335,000 μW), about 20× higher than we measured for *T. dichotomus*. However, they used quite wet soils with high thermal conductivities (0.3 – 0.5 $W{\cdot}°C^{-1}{\cdot}m^{-1}$) (Seymour and Bradford, 1992) and held the eggs in small volumes of soil in the lab such that heat was lost in all directions, both of which would elevate rates of heat loss. In addition, they measured surface rather than core temperatures. Thus, their data do not provide a strong test of the model predictions we developed. Better tests would measure core temperatures of larvae released into the wild, perhaps with small temperature loggers implanted in their hemocoels.

For hypothetical large insect larvae, in the range of 1 – 2 kg, the model suggests self-heating of about 1.5 – 6 °C, with the largest values coming from the largest larvae in the hottest, driest soils. Interestingly, larval *T. dichotomus* move toward CO_2 signals in the soil, which has two consequences for their distributions (Kojima et al., 2014). First, CO_2 emitted from fermenting soils (Kojima, 2015) may attract larvae to patches of soil with locally elevated rates of respiration, which are likely also to be warmer than surrounding patches. Second, CO_2 from conspecifics can be sensed by other larvae, causing them to aggregate into larger groups (Kojima, 2015). Although their complicated geometry violates many of the assumptions of our simple model, such aggregations may increase the local mass of heat-producing larval tissues enough to make self-heating more likely.

Would self-heating—either by groups of larvae or by hypothetical gigantic larvae—help or hurt larval performance? Although insects living in cool environments can potentially perform better by finding ways to warm up, this effect is unlikely to be important for underground larvae of beetles. First, because low soil temperatures depress metabolic heat production, larvae in cool conditions are the least likely to self-heat significantly. Second, cooler conditions often are associated with precipitation, which would moisten soil, increase soil thermal conductivity, and further reduce the steady-state larval temperature excess. It is easier to construct the argument that self-heating is harmful, from the converse of the statements above: self-heating is greatest in the warmest soils, and it occurs more readily in dry soils, which are likely to be associated with warmer, drier weather. Larval CT_{max} is high enough, however, that self-heating is very unlikely to push body temperatures to dangerous levels. It is more likely to push body temperatures above the temperature preferred by larvae on the thermal gradient bar (~29 °C). Clearly, larvae in that situation are capable of moving to cooler areas.

Many insects are highly effective behavioral thermoregulators. A behavioral approach to thermoregulation exploits locally available microclimates to obtain desired body temperatures, or at least to avoid extremes. Endothermic vertebrates obviously complement behavioral approaches with physiological strategies that exploit metabolic heat to attain high, stable body temperatures. Besides large flying insects, do any other insects use the vertebrate-like strategy of thermoregulating by controlling the production and loss of metabolic heat? We examined this question using large beetle larvae that live in soil. Our results suggest that their rates of heat production are too low, and rates of heat loss too high, to achieve more than a few degrees of self-heating under common sets of conditions. Thus, even the largest insect larvae still must rely on behavioral thermoregulation alone.

Author Contributions

NLC, DJE, and HAW conceived and designed the experiments. NLC performed the experiments, and NLC and HAW developed and analyzed the model. NLC and HAW analyzed the data. NLC and HAW wrote the manuscript, and DJE provided editorial advice.

Acknowledgments

This work was supported by the University of Montana and a Davidson Honors College Undergraduate Research Award. Thanks to Jon Harrison for critical comments on an earlier draft, and to John Terblanche for advice on thermal ramps. A special thanks to Warren Porter for detailed and helpful critiques of an earlier version of the heat-balance model. We also thank two anonymous reviewers for constructive comments on the manuscript.

Appendix A. Supporting information

Supplementary data associated with this article can be found in the online version at doi:10.1016/j.jtherbio.2016.10.002.

References

Ahn, H.K., Sauer, T.J., Richard, T.L., Glanville, T.D., 2009. Determination of thermal properties of composting bulking materials. Bioresour. Technol. 100, 3974–3981. http://dx.doi.org/10.1016/j.biortech.2008.11.056.

Bakken, G.S., 1992. Measurement and application of operative and standard operative temperatures in ecology. Am. Zool. 32, 194–216. http://dx.doi.org/10.1093/icb/32.2.194.

Bartholomew, G.A., Casey, T.M., 1978. Oxygen consumption of moths during rest, pre-flight warm-up, and flight in relation to body size and wing morphology. J. Exp. Biol. 76, 11–25.

Bird, R.B., Stewart, W.E., Lightfoot, E.N., 2002. Transport Phenomena 2nd edition. Wiley, New York.

Campbell, R., Phene, C., 1977. Tillage, Matric potential, oxygen and millet yield relations in a layered soil. Trans. ASAE 20, 271–275. http://dx.doi.org/10.13031/2013.35540.

Casey, T.M., 1981. Energetics and thermoregulation of *Malacosoma americanum* (Lepidoptera: lasiocampidae) during hovering flight. Am. Zool. 54, 362–371. http://dx.doi.org/10.1086/physzool.54.3.30159950.

Chown, S.L., Marais, E., Terblanche, J.S., Klok, C.J., Lighton, J.R.B., Blackburn, T.M., 2007. Scaling of insect metabolic rate is inconsistent with the nutrient supply network model. Funct. Ecol. 21, 282–290. http://dx.doi.org/10.1111/j.1365-2435.2007.01245.x.

Church, N.S., 1960. Heat loss and the body temperatures of flying insects II. Heat conduction within the body and its loss by radiation and convection. J. Exp. Biol. 37, 186–213.

Colinet, H., Renault, D., 2012. Metabolic effects of CO_2 anaesthesia in *Drosophila melanogaster*. Biol. Lett. 8, 1050–1054. http://dx.doi.org/10.1098/rsbl.2012.0601.

Deutsch, C.A., Tewksbury, J.J., Huey, R.B., Sheldon, K.S., Ghalambor, C.K., Haak, D.C., Martin, P.R., 2008. Impacts of climate warming on terrestrial ectotherms across latitude. Proc. Natl. Acad. Sci. USA 105, 6668–6672. http://dx.doi.org/10.1073/pnas.0709472105.

Emlen, D.J., Warren, I.A., Johns, A., Dworkin, I., Lavine, L.C., 2012. A mechanism of extreme growth and reliable signaling in sexually selected ornaments and weapons. Science 337, 860–864. http://dx.doi.org/10.1126/science.1224286.

Gates, D.M., 1980. Biophysical Ecology. Springer-Verlag, New York.

Greenlee, K.J., Harrison, J.F., 2005. Respiratory changes throughout ontogeny in the tobacco hornworm caterpillar, *Manduca sexta*. J. Exp. Biol. 208, 1385–1392. http://dx.doi.org/10.1242/jeb.01521.

Greenway, H., Armstrong, W., Colmer, T., 2006. Conditions leading to high CO_2 (> 5 kPa) in waterlogged-flooded soils and possible effects on root growth and metabolism. Ann. Bot. 98, 9–32. http://dx.doi.org/10.1093/aob/mcl076.

Harrison, J.F., Klok, C.J., Waters, J.S., 2014. Critical PO_2 is size-independent in insects: implications for the metabolic theory of ecology. Curr. Opin. Insect Sci. 4, 54–59. http://dx.doi.org/10.1016/j.cois.2014.08.012.

Heinrich, B., 1970. Thoracic temperature stabilization by blood circulation in a free-flying moth. Science 168, 580–582. http://dx.doi.org/10.1126/science.168.3931.580.

Heinrich, B., 1971a. Temperature regulation of sphinx moth, *Manduca sexta*. 1. Flight energetics and body temperature during free and tethered flight. J. Exp. Biol. 54, 141–152.

Heinrich, B., 1980. Mechanisms of body-temperature regulation in honey bees, *Apis mellifera*. II. Regulation of thoracic temperature at high air temperatures. J. Exp. Biol. 85, 73–87.

Heinrich, B., 1993. The Hot-Blooded Insects: Strategies and Mechanisms of Thermoregulation. Harvard University Press, Cambridge, MA.

Hongo, Y., 2007a. Evolution of male dimorphic allometry in a population of the Japanese horned beetle *Trypoxylus dichotomus septentrionalis*. Behav. Ecol. Sociobiol. 62, 245–253.

Hongo, Y., 2007b. Male–male combats of the Japanese horned beetle *Trypoxylus dichotomus septentrionalis*. Nat. Insects 42, 19–22, (In Japanese).

Karino, K., Seki, N., Chiba, M., 2004. Larval nutritional environment determines adult size in Japanese horned beetles *Allomyrina dichotoma*. Ecol. Res. 19 (6), 663–668.

Kingsolver, J.G., Woods, H.A., 1997. Thermal sensitivity of growth and feeding in *Manduca sexta* caterpillars. Physiol. Zool. 70, 631–638. http://dx.doi.org/10.1086/515872.

Kojima, W., 2015. Attraction to carbon dioxide from feeding resources and conspecific neighbours in larvae of the rhinoceros beetle *Trypoxylus dichotomus*. PLoS One 10 (11), 1. http://dx.doi.org/10.1371/journal.pone.0141733.

Kojima, W., Ishikawa, Y., Takanashi, T., 2014. Chemically mediated group formation in soil-dwelling larvae and pupae of the beetle *Trypoxylus dichotomus*. Naturwissenschaften 101, 687–695.

Kojima, W., Takanashi, T., Ishikawa, Y., 2012. Vibratory communication in the soil: pupal signals deter larval intrusion in a group-living beetle *Trypoxylus dichotoma*. Behav. Ecol. Sociobiol. 66, 171–179.

Lighton, J., Turner, R., 2004. Thermolimit respirometry: an objective assessment of critical thermal maxima in two sympatric desert harvester ants, *Pogonomyrmex rugosus* and *P. californicus*. J. Exp. Biol. 207, 1903–1913. http://dx.doi.org/10.1242/jeb.00970.

Macgregor, S.T., Miller, F.C., Psarianos, K.M., Finstein, M.S., 1981. Composting process control based on interaction between microbial heat output and temperature. Appl Environ. Microbiol 41, 1321–1330.

May, M.L., 1979. Insect Thermoregulation. Ann. Rev. Entomol. 24, 313–349. http://dx.doi.org/10.1146/annurev.en.24.010179.001525.

McCullough, E.L., 2012. Using radio telemetry to assess movement patterns in a giant rhinoceros beetle: are there differences among majors, minors, and females? J. Insect Behav. 2012, 1–6.

Plaistow, S.J., Tsuchida, K., Tsubaki, Y., Setsuda, K., 2005. The effect of a seasonal time constraint on development time, body size, condition, and morph determination in the horned beetle *Allomyrina dichotoma* L.(Coleoptera: scarabaeidae). Ecol. Entomol. 30, 692–699.

Prange, H.D., 1996. Evaporative cooling in insects. J. Insect Physiol. 42, 493–499. http://dx.doi.org/10.1016/0022-1910(95)00126-3.

Rezende, E.L., Tejedo, M., Santos, M., 2011. Estimating the adaptive potential of critical thermal limits: methodological problems and evolutionary implications. Funct. Ecol. 25, 111–121.

Robinson, W.R., Peters, R.H., Zimmermann, J., 1983. The effects of body size and temperature on metabolic rate of organisms. Can. J. Zool. 61, 281–288. http://dx.doi.org/10.1139/z83-037.

Schmidt-Nielsen, K., 1997. Animal Physiology: Adaptation and Environment 5th edition. Cambridge University Press, Cambridge.

Seymour, R.S., Bradford, D.F., 1992. Temperature regulation in the incubation mounds of the Australian brush-turkey. Condor 94, 134–150.

Seymour, R.S., Vleck, D., Vleck, C.M., Booth, D.T., 1987. Water relations of buried eggs of mound building birds. J. Comp. Physiol. B 157, 413–422.

Soetaert, K., Petzoldt, T., Setzer, R.W., 2010. Solving differential equations in R: package deSolve. J. Stat. Softw. 33, 1–25 . http://dx.doi.org/10.18637/jss.v033.i09, (URL) ⟨http://www.jstatsoft.org/v33/i09/⟩.

Terblanche, J.S., Deere, J.A., Clusella-Trullas, S., Janion, C., Chown, S.L., 2007. Critical thermal limits depend on methodological context. Proc. R. Soc. B 274, 2935–2942. http://dx.doi.org/10.1098/rspb.2007.0985.

Vleck, D., Vleck, C.M., Seymour, R.S., 1984. Energetics of embryonic development in the megapode birds, mallee fowl *Leipoa ocellata* and brush turkey *Alectura lathami*. Physiol. Zool. 57, 444–456.

Westcot, D.W., Wierenga, P.J., 1974. Transfer of heat by conduction and vapor movement in a closed soil system. Soil Sci. Soc. Am. Proc. 38, 9–14.

Woods, H.A., Dillon, M.E., Pincebourde, S., 2015. The roles of microclimatic diversity and of behavior in mediating the responses of ectotherms to climate change. J. Therm. Biol. 54, 86–97. http://dx.doi.org/10.1016/j.jtherbio.2014.10.002.

Woodman, J.D., Cooper, P.D., Haritos, V.S., 2007. Cyclic gas exchange in the giant burrowing cockroach, *Macropanesthia rhinoceros*: effect of oxygen tension and temperature. J. Insect Physiol. 53, 497–504. http://dx.doi.org/10.1016/j.jinsphys.2007.01.012.

Xu, L., Snelling, E.P., Seymour, R.S., 2014. Burrowing energetics of the giant burrowing cockroach *Macropanesthia rhinoceros*: an allometric study. J. Insect Physiol. 70, 81–87. http://dx.doi.org/10.1016/j.jinsphys.2014.09.005.